



# Shanidar 3 'rings the bell': Virtual ribcage reconstruction and its implications for understanding the Neanderthal bauplan

José M. López-Rey <sup>a, b, \*</sup>, Daniel García-Martínez <sup>c, d, e</sup>, Markus Bastir <sup>a</sup>

<sup>a</sup> Paleanthropology Group, Department of Paleobiology, Museo Nacional de Ciencias Naturales (MNCN-CSIC), Calle José Gutiérrez Abascal, 2, 28006, Madrid, Spain

<sup>b</sup> Department of Biology, Faculty of Sciences, Universidad Autónoma de Madrid (UAM), Calle Darwin, 2, 28049, Madrid, Spain

<sup>c</sup> Physical Anthropology Unit, Faculty of Biological Sciences, Universidad Complutense de Madrid (UCM), Calle José Antonio Novais, 12, 28040, Madrid, Spain

<sup>d</sup> Laboratory of Forensic Anthropology, Centre for Functional Ecology, Department of Life Sciences, University of Coimbra (UC), Calçada Martim de Freitas, 3000-456, Coimbra, Portugal

<sup>e</sup> Centro Nacional de Investigación sobre la Evolución Humana (CENIEH), Paseo de la Sierra de Atapuerca 3, 09002, Burgos, Spain

## ARTICLE INFO

### Article history:

Received 1 July 2024

Accepted 21 November 2024

Available online 11 December 2024

Handling Editor: Dr A Taylor

### Keywords:

Thorax

Body proportions

Paleoenvironment

Geometric morphometrics

## ABSTRACT

The study of the ribcage is fundamental to understanding hominin evolution. However, ribs and vertebrae are scarce in the fossil record. Although Neanderthals are one of the most represented and, therefore, one of the most studied fossil *Homo* species, it is controversial whether there is a standardized Neanderthal ribcage morphotype that could differ from modern humans. Hence, we used three-dimensional geometric morphometrics to reconstruct and compare the Neanderthal ribcage of Shanidar 3 with another Neanderthal specimen, Kebara 2, and with 58 *Homo sapiens* individuals of worldwide distribution. Shape differences among the Neanderthal and *H. sapiens* ribcages were analyzed by a hierarchical cluster using the Euclidean distances among the permuted Procrustes distances between groups. Size differences between the Neanderthal and *H. sapiens* ribcages were examined using a permutation test on centroid size. To examine the potential for allometry, we performed a linear regression of Procrustes coordinates on centroid size of the sample, followed by a principal component analysis in form space. Our results show that Shanidar 3 has the 'bell-shaped' thorax typically described for Neanderthals. In fact, the shapes of both Shanidar 3 and Kebara 2 ribcages cluster apart from that of *H. sapiens*, being closer to cold-adapted individuals. The study of the centroid size supports similarities between Neanderthals and cold-adapted *H. sapiens* since significant size differences were found only between Neanderthals and temperate/tropical recent humans. The linear regression and principal component analysis showed an allometric relationship between ribcage size and shape, suggesting Neanderthals had larger and stockier ribcages than most *H. sapiens*, although they fall within the *H. sapiens* range of variation. Finally, ribcage similarities found between Shanidar 3 and Kebara 2, both inhabiting warm Levantine locations during the Upper Pleistocene, could challenge the conventional idea of a cold-adapted bauplan in Neanderthals.

© 2024 The Author(s). Published by Elsevier Ltd. This is an open access article under the CC BY-NC license (<http://creativecommons.org/licenses/by-nc/4.0/>).

## 1. Introduction

The study of the ribcage is crucial for understanding not only anatomical but also physiological, functional, and even behavioral traits in the context of hominin evolution. Throughout the last three decades, a comparative description of the *Australopithecus*

and *Homo* ribcages has elucidated differences among the species that might be intimately linked to variation in their ecosystems (Bastir et al., 2022). Hence, it has been proposed that the narrow upper thorax of *Australopithecus* was suitable for arboreality (Schmid et al., 2013), the stocky lower thorax of Neanderthals was helpful to avoid heat loss (Franciscus and Churchill, 2002; Weinstein, 2008; Gómez-Olivencia et al., 2009) or even to support an enlarged liver for protein processing (Ben-Dor et al., 2016), and the slender ribcage of *Homo sapiens* was highly efficient in the context of endurance running during persistence hunting (Bramble

\* Corresponding author.

E-mail address: [jlopezr@mncn.csic.es](mailto:jlopezr@mncn.csic.es) (J.M. López-Rey).

and Lieberman, 2004; Lieberman and Bramble, 2007; Pomeroy, 2023). However, the study of the ribcage in the fossil record is limited by the fact that vertebrae, and mainly ribs, are numerous and fragile. Therefore, costovertebral series tend to appear incomplete, broken, and/or commingled (Manifold, 2012; Schotsmans et al., 2017; Abdel-Maksoud et al., 2022), so there have been only a few attempts at hominin ribcage reconstructions in the literature (Sawyer and Maley, 2005; Gómez-Olivencia et al., 2018; Bastir et al., 2020; García-Martínez et al., 2020).

Among all extinct *Homo* species, the ribs and thoracic vertebrae of Neanderthals have been the most studied and compared to modern humans (Franciscus and Churchill, 2002; Weinstein, 2008; Gómez-Olivencia et al., 2009, 2018; Bastir et al., 2017a; García-Martínez et al., 2017, 2018a, 2018b, 2020). Despite this work, it remains controversial whether there are significant differences between the three-dimensional (3D) shapes of their ribs and, consequently, the 3D configuration of their thorax (Gómez-Olivencia et al., 2009). In general terms, it has been suggested that *Homo neanderthalensis*' ribs are more horizontally oriented and less declined (a reduced degree of rib lowering dependent on the position of the costovertebral joint [García-Martínez et al., 2016]) than those of *H. sapiens*, which would result in a relatively wider and deeper ribcage in Neanderthals, especially in the lower part (Franciscus and Churchill, 2002; Weinstein, 2008; Gómez-Olivencia et al., 2009; García-Martínez et al., 2014, 2017, 2018a, 2018b). Curiously, although Neanderthal ribs are longer, especially around the mid-thorax, Gómez-Olivencia et al. (2009, 2018) suggested that their 3D configuration within the thorax results in a ribcage volume that is not especially different from that of *H. sapiens*. Nevertheless, this model has only been supported by the virtual reconstruction of the Neanderthal adult thorax belonging to Kebara 2 (Gómez-Olivencia et al., 2018). Functionally, a 'bell-shaped' ribcage in Neanderthals (Sawyer and Maley, 2005) would potentially lead to a greater diaphragmatic action during breathing, as opposed to thoracic breathing more typical of the 'barrel-shaped' thorax of *H. sapiens* (López-Rey et al., 2023). These differences in breathing kinematics could have different biological implications that are detailed in the following.

It has been proposed that Neanderthals had a higher basal metabolic rate than *H. sapiens*, which would support a higher energetic demand derived from their larger body mass index (Churchill, 2006). To maintain their high basal metabolic rate, Neanderthals would have needed a higher oxygen supply, which is in line with the larger respiratory system estimated for Neanderthals (e.g., greater cranial airways: Bastir, 2008; greater lung capacity: García-Martínez et al., 2018b). Other authors state that these features could also have been involved in thermoregulation, given the cold climate conditions in which Neanderthals supposedly lived during the Upper Pleistocene (Churchill, 2006; Weinstein, 2008; Ocozbek et al., 2021). Additionally, higher activity rates proposed for Neanderthals have been tentatively linked to ambush hunting strategies, where explosive strength (e.g., Ayalon et al., 1974) is required, rather than the endurance proposed for *H. sapiens* hunter-gatherers (Bramble and Lieberman, 2004; Lieberman and Bramble, 2007; Raichlen et al., 2011; Stewart et al., 2019; Pomeroy, 2023). However, it has been argued that the robust bauplan proposed for Neanderthals 1) could not have been strictly adapted to climate or diet (Weaver et al., 2007; Weaver, 2009; Henry et al., 2011; Hardy et al., 2022) and 2) might be included in the recent *H. sapiens* range of variation (Arensburg, 1991), given the worldwide distribution of the latter and their ecogeographic adaptations to different environments (López-Rey et al., 2024a).

To shed light on this issue, we performed a 3D reconstruction of the ribcage belonging to Shanidar 3, an adult Neanderthal specimen from Iraq. This individual is important in the context of Neanderthal ribcage anatomy because its ribs are well preserved

and have already been extensively studied. Thus, previous research has already provided a two-dimensional assessment of the shape of the Shanidar 3 thorax (Franciscus and Churchill, 2002). In addition, Kebara 2 and Shanidar 3 share a similar location (as both are Levantine Neanderthals), similar dating (45–60 ka BP) and, therefore, similar paleoenvironment (milder, in contrast with Northwestern Europe; Franciscus and Churchill, 2002; Gómez-Olivencia et al., 2009; Frumkin et al., 2011; Müller et al., 2011; Helmens, 2014; Bar-Matthews et al., 2019; Pomeroy et al., 2020). With this in mind, we propose the following hypotheses:

1. The ribcage of Shanidar 3 has the typical Neanderthal 'bell-shaped' configuration seen in Kebara 2, that is, with an anteroposteriorly and mediolaterally expanded lower thorax compared to *H. sapiens* (Gómez-Olivencia et al., 2018).
2. There are no differences in ribcage size between Neanderthals and *H. sapiens*. Although Neanderthal ribs are longer, especially around the mid-thorax, their 3D configuration within the thorax makes ribcage volume such as that of modern humans (Gómez-Olivencia et al., 2009, 2018).

## 2. Materials and methods

The sample gathered for this study consists of the ribs and vertebrae belonging to the two Neanderthal adult specimens, Shanidar 3 and Kebara 2, and 58 recent adult male *H. sapiens* of worldwide distribution (Table 1). Fossil costovertebral remains of Shanidar 3 were scanned using computed tomography (CT) at their host institution, the Smithsonian National Museum of Natural History (Washington, DC., USA), whereas remains belonging to Kebara 2 (housed at Tel Aviv University, Israel) were CT-scanned at Mount Carmel Medical Center (Haifa, Israel). In addition, costovertebral material from recent humans was obtained using CT scans and surface scans, as specified in the Supplementary Online Material (SOM) Table S1. All the virtual rib and vertebra models were postprocessed in Artec Studio v. 16 ([www.artec3d.com](http://www.artec3d.com)) for cleaning, smoothing edges, and filling possible gaps.

We first estimated the missing elements of the Shanidar 3 costovertebral material following the protocol developed by García-Martínez et al. (2018c). Briefly, we used the Artec Spider scanner ([www.artec3d.com](http://www.artec3d.com)) to create virtual models of the costovertebral remains belonging to a control sample of 10 present-day adult male *H. sapiens* housed at the Faculty of Medicine, Universidad Complutense de Madrid. We then quantified the size and shape from these scans, using a specific template for ribs and another one for vertebrae. Next, we calculated the vector of change between each mean metamer as the increment of 3D coordinates between each costovertebral level and the subsequent one. For example, we calculated the mean coordinates of ribs 5 and 6 for our control sample. We then subtracted the coordinates belonging to rib 6 from those belonging to rib 5. The obtained values represent the vector of change between ribs 5 and 6. If we add this vector to the coordinates of the fifth rib belonging to the specimen of study, we would 'force' it to become a sixth rib. By contrast, if we subtract this vector from the sixth rib of the specimen of study, we would 'force' this rib to become a fifth one. Hence, this vector was added or subtracted to the best-preserved costovertebral levels of Shanidar 3, depending on whether we wanted to estimate missing elements below or above the level, respectively. Eventually, the obtained coordinates were morphed, and the final meshes were obtained, adding the preserved fossil material of Shanidar 3 to the estimated volumes.

The estimated ribs and vertebrae of Shanidar 3 were disarticulated. Thus, it was necessary to perform a 3D reconstruction of the ribcage. To make an accurate reconstruction of the Shanidar 3

**Table 1**  
Demographic information about the *Homo sapiens* sample extracted from López-Rey et al. (2024a).

Ancestry	Population	Site	Number of individuals	Latitude (approximate)	Annual average temperature (approximate)	Datation (centuries)	Climate
Native North American	Inuit	Point Hope, Alaska (USA)	3	70°	≤-2 °C	13th–17th	Cold
Native North American	Inuit	Greenland (Denmark)	3	68°	≤-2 °C	13th–18th	
North European	Norsemen	Nuuk, Greenland (Denmark)—Scandinavian origin	2	64°	≤7 °C	11th–15th	
Native South American	South Patagonian–Fuegian	Isla Grande de Tierra del Fuego (Argentina/Chile)	3	-53°	5 °C	17th–20th	Temperate
Western European	French	Paris (France)	3	48°	11 °C	20th	
Southern European	Spanish	Madrid (Spain)	3	40°	15 °C	20th	
Native North American	—	New Mexico (USA)	3	35°	16 °C	21st	
Native North American	Niminokotche, Chumash, Alapakassil	California (USA)	2	34°	19 °C	—	
Yamato	Japanese	Hyōgo Prefecture (Japan)	3	34°	16 °C	—	
Native Canarian	Canarian	Gran Canaria, Canary Islands (Spain)	5	28°	23 °C	—	Tropical
Latinamerican	Mexican	Mexico	3	25°	19 °C	21st	
Native South American	—	Santiago del Estero (Argentina)	3	-27°	23 °C	—	
Native South American	North Patagonian	Río Negro and Chubut (Argentina)	4	-41°	11 °C	—	
North African	Nubian	Abri, Northern State (Sudan)	3	21°	≥25 °C	3rd–1st b.C.	
Native Southeastern Asian	Negrito	Luzon (Philippines)	3	15°	27 °C	—	
Melanesian	Papuan	New Britain (Papua New Guinea)	3	-6°	27 °C	—	
Native South American	—	Ancón (Peru)	3	-9°	21 °C	16th	
Sub-Saharan	—	Lagos (Portugal)—Subsaharan origin	3	15° to -20°	≥25 °C	15th–17th	
Sub-Saharan	Afro-American	New Mexico (USA)—Subsaharan origin	3	15° to -20°	≥25 °C	21st	

ribcage, we followed the standardized protocol developed by López-Rey et al. (2024b). We first calculated the theoretical thoracic kyphosis of this specimen using the 'thoracic vertebral body height difference' (TVBHD) method (Been et al., 2019). This method consists of measuring the anterior (A) and posterior (P) vertebral body heights from T1 to T12 and dividing their sum to obtain the A–P ratio. Then the A–P ratio is included in a regression formula ( $297.114 - 272.31 \times A-P$  ratio), with the result being the approximate angle of thoracic kyphosis in males (Table 2). Then we reconstructed the thoracic spine by the corrected 'zygapophyseal facet method' (Bastir et al., 2019), which consisted of preserving contiguity and maximal overlap of the zygapophyseal facets, taking into consideration the wedging of the vertebral body. Once the spine was reconstructed, we placed the ribs in their corresponding place, maintaining their expected position in functional residual

**Table 2**  
Estimated thoracic kyphosis for Shanidar 3 using the TVBHD method.

Shanidar 3		
Vertebra	Anterior height (mm)	Posterior height (mm)
T1	15.26	17.17
T2	16.49	18.1
T3	16.85	18.14
T4	17.32	19.44
T5	18.2	20.76
T6	18.81	20.31
T7	19.49	21.3
T8	18.69	20.7
T9	19.2	23.68
T10	19.58	22.98
T11	21.6	24.86
T12	22.27	25.41
Sum	223.76	252.85
A–P ratio <sup>a</sup>	0.885	
Estimated kyphosis (°)	56.13	

TVBHD = thoracic vertebral body height difference; A = anterior; P = posterior.

<sup>a</sup> Ratio of the sum of the anterior to posterior height of the vertebral bodies.

capacity (Wanger et al., 2005). For the remainder of the sample, 3D ribcage models belonging to Kebara 2 and the comparative *H. sapiens* remains were already reconstructed by Gómez-Olivencia et al. (2018) and López-Rey et al. (2024a), respectively (Fig. 1).

The size and shape of the full sample were quantified in Viewbox v. 4.1 (<https://www.dhal.com/viewbox.htm>) using a template of 526 (semi)landmarks, which was previously described by Bastir et al. (2017b). Before statistical analyses, we excluded the coordinates from ribs 11 and 12 since these ribs are highly variable in form (Gómez-Olivencia et al., 2009) and could introduce noise in the analysis and interpretation of the results. We also symmetrized each ribcage to avoid the impact of morphological alterations, such as scoliosis, in our analyses. Overall shape differences among the ribcage of Neanderthals and *H. sapiens* (divided into three climatic groups based on latitude, cold, temperate, and tropical; López-Rey et al., 2024a) were tested using a permutation test (10,000 permutations) on the mean Procrustes distances between groups. The Euclidean distances among these permuted Procrustes distances were used to subsequently perform a hierarchical cluster analysis among groups (Fig. 2). Size differences between the Neanderthal and *H. sapiens* ribcages were evaluated using permutation tests (10,000 permutations) on their centroid size (Table 3), which are depicted in a boxplot in Figure 3. The potential for allometry was tested using a linear regression (Fig. 4) of the Procrustes coordinates on the centroid size of the full sample (all *H. sapiens* plus Shanidar 3 and Kebara 2) and a principal components analysis (PCA) in form space (no scaling). Statistical differences in principal component 1 (PC1), PC2, and PC3 scores between Neanderthals and *H. sapiens* were evaluated using permutation tests (10,000 permutations). Graphically, the distribution of these scores was displayed by two scatterplots (PC1–PC2 and PC1–PC3; Fig. 5). All statistical analyses were performed in RStudio v. 2023.12.1–402 (R Core Team, 2023) using the packages 'geomorph' v. 4.04 (Adams et al., 2022), 'ggplot2' v. 3.3.3 (Wickham, 2016), 'Morpho' v. 2.10, 'Rvcg' v. 0.22.1 (Schlager, 2017), and 'stats' v. 4.2.3 (R Core Team, 2023). The full R script is included in SOM S1.

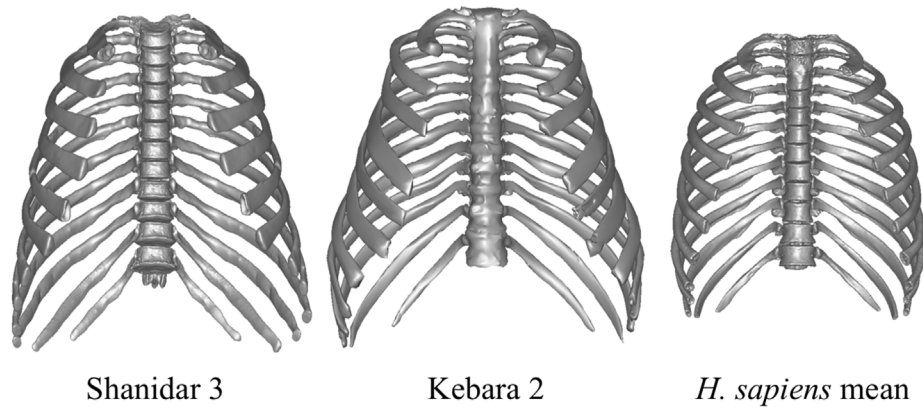


Figure 1. Frontal view of the 3D models of the ribcages belonging to Shanidar 3, Kebara 2, and the *Homo sapiens* mean. 3D = three-dimensional.

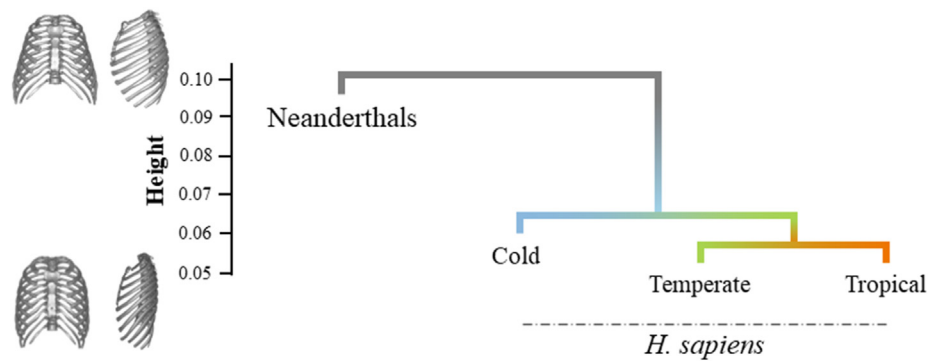


Figure 2. Hierarchical cluster on the Euclidean distances among the permuted mean Procrustes distances between Neanderthals and *Homo sapiens*.

### 3. Results

The thoracic kyphosis of Shanidar 3 was estimated at approximately 56.13° degrees of curvature by the TVBHD method (Table 2). Therefore, thoracic vertebrae were positioned in such a way that the obtained kyphosis angle was the closest to that value. Then ribs were placed on the reconstructed spine, obtaining a 3D model of the Shanidar 3 ribcage that can be downloaded and visualized freely using the following links: <https://digital.csic.es/handle/10261/372005> and <https://hdl.handle.net/20.500.14352/110866>. Figure 1 shows that the reconstructed ribcage of Shanidar 3 has the expanded lower thorax typical of Neanderthals, such as Kebara 2. Based on the hierarchical cluster analysis, Neanderthals are the outgroup, whereas the cold-adapted *H. sapiens* are closest to the Neanderthal ribcage 3D configuration (Fig. 2). In addition, the Neanderthal ribcage is significantly larger ( $p < 0.05$ ) than that of the full *H. sapiens* sample. However, if we repeat the analysis of centroid size for the recent human sample according to latitude, we find that

1) there are no statistical differences between Neanderthals and cold-adapted *H. sapiens* and 2) centroid size of Neanderthals falls outside the range of centroid size of tropical *H. sapiens* (Fig. 3; Table 3).

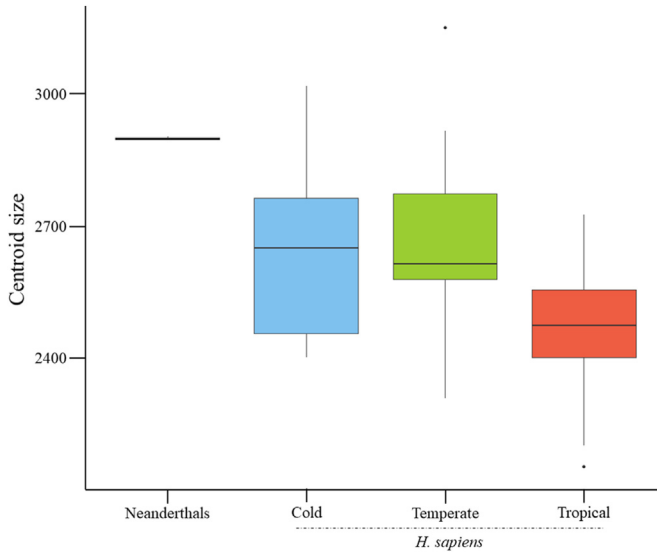
The linear regression of Procrustes coordinates on centroid size was significant ( $p < 0.05$ ) and showed that stocky ribcages are significantly larger than slender ribcages (Fig. 4). Although the Neanderthal ribcages of Shanidar 3 and Kebara 2 are similar in size, Figure 4 suggests that the latter is stockier. Regarding the PCA, both Shanidar 3 and Kebara 2 are included in the *H. sapiens* range of variation but located in the margins of the plots (Fig. 5). Even though we found significant differences ( $p < 0.05$ ) between Neanderthals and the full *H. sapiens* sample for PC1 (41.85% of total form variation,  $p = 0.039$ ), there were no significant differences for PC2 (12.39% of total form variation,  $p = 0.79$ ) or PC3 (10.81% of total form variation,  $p = 0.19$ ). Nevertheless, when the *H. sapiens* sample was grouped according to latitude, statistical differences between groups at PC1 were only significant between Neanderthals and

Table 3

Statistical analysis of the centroid size between Neanderthals and *Homo sapiens* (both full sample and separated by latitude).

	Statistics	Neanderthals	<i>Homo sapiens</i> (full sample)	Neanderthals	<i>Homo sapiens</i>			
					Cold	Temperate	Tropical	
Mean ± SD	Mean	2899.5	2598.5	2899.5	2636.1	2663.1	2471.3	
	SD	5.9	190.4	5.9	192.8	176.2	152.8	
Permutations test (10,000 permutations)	p-value	<b>0.03<sup>a</sup></b>		0.1	–	–	–	Cold <i>Homo sapiens</i>
				<b>0.04<sup>a</sup></b>	0.50	–	–	Temperate
				<b>0.01<sup>a</sup></b>	<b>0.04<sup>a</sup></b>	<b>0.03<sup>a</sup></b>	–	Tropical

SD = standard deviation.  
<sup>a</sup> Significant at  $p < 0.05$ .



**Figure 3.** Boxplots comparing the centroid size of the Neanderthals and the *Homo sapiens* sample grouped by latitude. Neanderthals are significantly larger ( $p < 0.05$ ) than tropical and temperate *H. sapiens*, but no differences were found between them and cold-adapted *H. sapiens*.

tropical *H. sapiens* ( $p = 0.01$ ). Principal component 1 shows variation in ribcage size and shape (negative = larger and more pyramidal; positive = smaller and more globular); PC2 shows different degrees of rib declination (negative = higher declination; positive = lower declination); and PC3 describes how rib torsion affects ribcage depth (negative = higher torsion and lower depth, positive = lower torsion and greater depth). If we interpret the distribution of the PC scores for each group, it can be noticed that the Neanderthal ribcage is larger and more pyramidal than the *H. sapiens* ribcage. Furthermore, although there are no differences

in rib declination, ribs have less torsion in Neanderthals than in *H. sapiens*, which results in a deeper thorax in Neanderthals (Fig. 5).

#### 4. Discussion

This study presents a standardized reconstruction of the Shanidar 3 ribcage and describes its morphology compared to *H. sapiens* and another Neanderthal specimen, Kebara 2. Our estimate of the thoracic kyphosis of Shanidar 3 using the zygopophyseal facet method + TVBHD method resulted in a curvature of  $56.13^\circ$  (Table 2). This value is close to what is expected for *H. sapiens* ( $\approx 50^\circ$ ) but far from the thoracic kyphosis calculated for Kebara 2 ( $44^\circ$ ) by Been et al. (2019). We hypothesize that this difference might be a consequence of 1) the missing element estimation method (García-Martínez et al., 2018); 2) intraspecific variability; or 3) age. Thoracic kyphosis can increase with aging (Zappalá et al., 2021), and estimations suggest that Kebara 2 was  $32 \pm 7$  years of age (Karasik et al., 1998), whereas Shanidar 3 was  $41 \pm 6.7$  years of age (Trinkaus and Thompson, 1987). Regarding the full ribcage reconstructions shown in Figure 1, Shanidar 3 and Kebara 2 share the 'bell-shaped' thorax associated with Neanderthals (Sawyer and Maley, 2005), whose lower part is mediolaterally and anteroposteriorly expanded compared to *H. sapiens* (Franciscus and Churchill, 2002; Weinstein, 2008; Gómez-Olivencia et al., 2009, 2018; García-Martínez et al., 2017, 2018a, 2018b). As stated in the literature, the thoracic morphotype described for Shanidar 3 and Kebara 2 is characterized by larger and more horizontal ribs than recent humans, along with greater bone robusticity (Franciscus and Churchill, 2002; Gómez-Olivencia et al., 2009, 2018). This Neanderthal 'bell-shaped' ribcage would be integrated into a torso whose pelvis is relatively wider and more flared than in *H. sapiens*, presumably determining a stockier bauplan in Neanderthals (Sawyer and Maley, 2005; Gómez-Olivencia et al., 2018; Pomeroy, 2023).

In terms of ribcage shape, differences described between Neanderthals and *H. sapiens* are confirmed in Figure 2 since

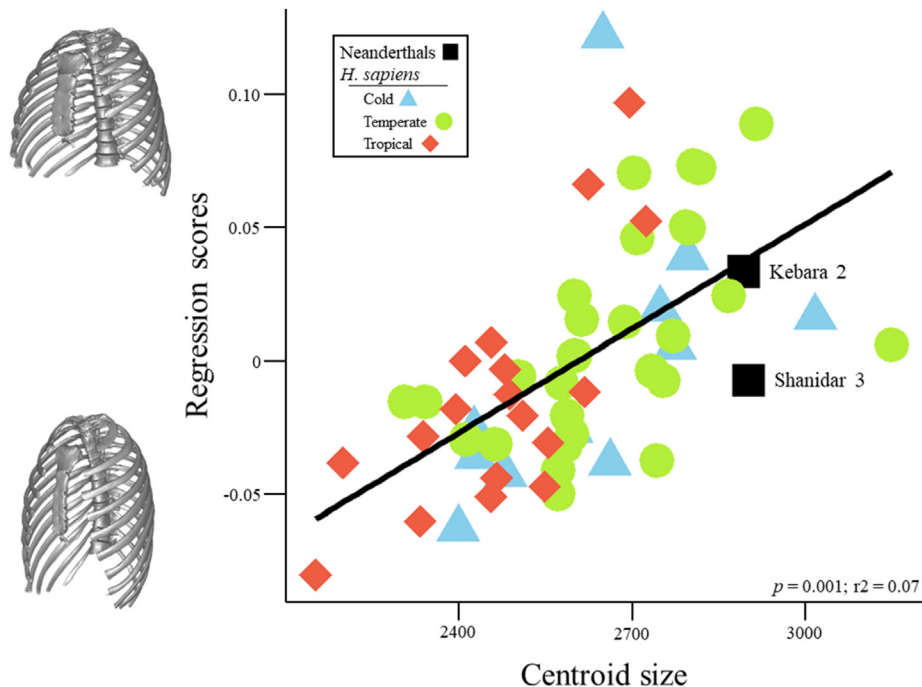


**Figure 4.** Linear regression of shape (regression scores on Procrustes coordinates) and size (centroid size) for the full sample.

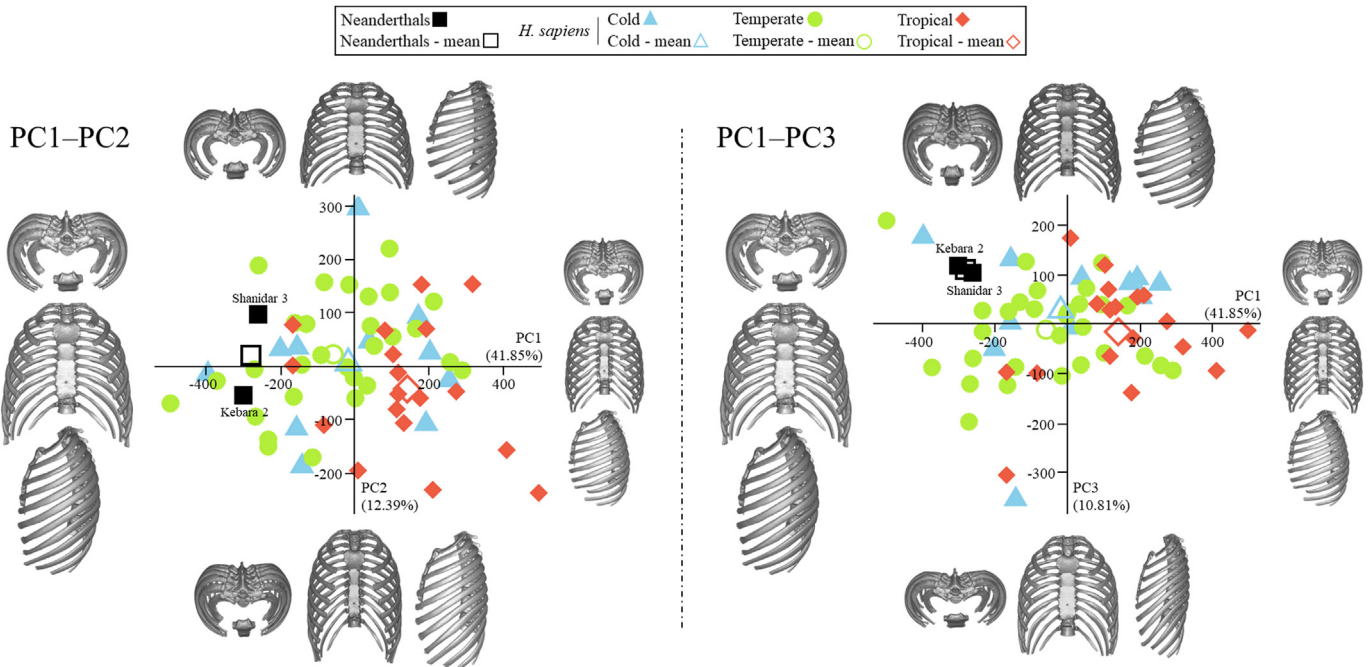


**Figure 5.** Scatterplots representing the distribution of the principal component 1 (PC1), PC2, and PC3 scores. Mean coordinates of each group are also included as empty symbols. Visualizations show shape plus size of the ribcage at both extremes of the axes.

Neanderthals fall outside the modern human cluster and form an outgroup. This might support our first hypothesis, which proposed that Shanidar 3 would have a ribcage shape like Kebara 2 and, consequently, different from *H. sapiens*. Interestingly, cold-adapted *H. sapiens* have the closest ribcage to Neanderthals, something previously described for isolated ribs (Gómez-Olivencia et al., 2009). On the one hand, this could indicate potential anatomical adaptations to a cold environment (Franciscus and Churchill, 2002; Weinstein, 2008; Gómez-Olivencia et al., 2009) or a high protein diet (Ben-Dor et al., 2016) shared by both Neanderthals and cold-adapted *H. sapiens*. On the other hand, genetic drift (Franciscus and Churchill, 2002) and equifinality, which describes an anatomical convergence driven by different evolutionary paths (Churchill, 2006), could be factors driving these ribcage similarities. In terms of size, the Neanderthal ribcage is significantly larger (centroid size = 2899.5 ± 5.9) than the *H. sapiens* ribcage (2598.5 ± 190.4; Table 3). A priori, this finding contradicts our second hypothesis, which proposed that there are no size differences between Neanderthals and recent humans (Gómez-Olivencia et al., 2009, 2018). However, if we separate the *H. sapiens* sample into groups corresponding to latitudinal areas and calculate their average centroid size, tropical individuals are notably smaller than the rest (Fig. 3; Table 3). It seems that including these populations increases the variance of the *H. sapiens* sample and results in significant size differences when we compare the full recent human sample to Neanderthals. Curiously, when we separate the *H. sapiens* individuals into latitudinal groups, the ribcage size of cold-adapted *H. sapiens* is not significantly different from that of Neanderthals ( $p > 0.05$ ; Table 3). This strengthens what was discussed previously for ribcage shape (Fig. 2) and suggests that cold-adapted *H. sapiens* have the closest ribcage morphology to Neanderthals among the other modern human populations in our sample. These results also highlight the importance of gathering a worldwide and diverse control sample in paleoanthropological studies.

Our linear regression displayed a significant correlation between size and shape, such that larger ribcages are stockier than smaller

ones (Fig. 4). This is consistent with the study by López-Rey et al. (2024a) and shows that Neanderthals have larger and stockier ribcages than most of the *H. sapiens* sample, especially in comparison to individuals from tropical environments. Nevertheless, this linear regression shows that the ribcage of Shanidar 3 is not as stocky as that of Kebara 2. Apart from potential intraspecific variation or the effect of Shanidar 3's pronounced thoracic kyphosis (Table 2), we suggest that this difference could be an artifact of the reconstruction method used for this Neanderthal specimen since the reference individuals were present-day humans (García-Martínez et al., 2018; see section 2, paragraph two). Regarding the PCA (Fig. 5), significant differences ( $p < 0.05$ ) between Neanderthals and *H. sapiens* were only found for PC1. However, when separating the recent human sample according to latitude, differences were significant only between Neanderthals and tropical individuals ( $p = 0.01$ ). This result suggests that the Neanderthal ribcage is larger and more pyramidal than those of recent humans, particularly when compared to tropical individuals, as evidenced by the mean coordinates of each group at PC1. Principal component 2 ( $p > 0.05$ ) shows that *H. sapiens* rib declination is quite variable and encompasses that of Neanderthals. Principal component 3, also not significantly different ( $p > 0.05$ ) between Neanderthals and *H. sapiens*, is in line with previous research that shows lower rib torsion in Shanidar 3 and Kebara 2 compared to recent humans (Franciscus and Churchill, 2002; Weinstein, 2008; Gómez-Olivencia et al., 2009, 2018; García-Martínez et al., 2017, 2018a, 2018b). Importantly, this PC also shows that anteroposterior depth is a specific—and possibly primitive—feature of the Neanderthal ribcage (Gómez-Olivencia et al., 2018; García-Martínez et al., 2020; Bastir et al., 2020).

The anatomical differences between the Neanderthal and *H. sapiens* ribcages described previously might also indicate functional differences in terms of breathing. In fact, previous research proposed that the 'bell-shaped' Neanderthal ribcage might have constrained rib sagittal elevation, given its lower rib torsion in relation to modern humans (Gómez-Olivencia et al., 2018). By contrast, the diaphragmatic surface would be larger in

Neanderthals than in *H. sapiens* since their lower thorax is relatively more expanded (López-Rey et al., 2023). Both characteristics suggest that breathing kinematics in Neanderthals may rely more on diaphragmatic contraction in contrast to *H. sapiens*, where rib movements in the sagittal plane are also crucial during breathing (Graeber and Nazim, 2007; LoMauro and Aliverti, 2018). Also, in vivo kinematic simulations have shown that volumetric variations in the lower thorax produce much greater variations in lung volumes than those produced in the upper thorax (Bastir et al., 2017b), which would provide further support for the idea of a larger respiratory system in Neanderthals (Franciscus and Churchill, 2002; Bastir, 2008, 2019b; García-Martínez et al., 2018b). Thus, the Neanderthal respiratory system would allow greater oxygen supply, leading to higher activity rates that would tentatively be suitable to ambush hunting strategies where explosive strength is required, rather than the endurance proposed for *H. sapiens* hunter-gatherers (Bramble and Lieberman, 2004; Lieberman and Bramble, 2007; Raichlen et al., 2011; Stewart et al., 2019; Pomeroy, 2023). Our results, however, have limitations related to the nature of geometric morphometric studies. By reducing the full anatomy of the ribcage to the geometry reflected by certain (semi)landmarks, discrete features that are evidently different in a visual examination of the remains are diluted in the statistical analyses (Richtsmeier et al., 2002; Bastir, 2018). Therefore, results derived from geometric morphometrics should always be accompanied by a detailed study of the original bones.

In the present case, regarding the reconstructed ribcage of Shanidar 3, we found visual and statistical differences with *H. sapiens* and similarities to Kebara 2 (Fig. 1). This holds relevance since it provides a new perspective on the traditional concept of the cold-adapted Neanderthal ribcage. According to the literature, climate during marine isotope stage (MIS) 4/early MIS 3 was as warm as it is today in the Levant but was extremely cold in Northwestern Europe (Müller et al., 2011; Helmens, 2014; Bar-Matthews et al., 2019). Additionally, it has been demonstrated that Neanderthals had a diverse diet in both locations (Henry et al., 2011; Hardy et al., 2022). Hence, our results on Levantine Neanderthals would support the idea that the robust 'bell-shaped' ribcage traditionally described for *H. neanderthalensis* was specifically adapted neither to cold conditions (Franciscus and Churchill, 2002; Weinstein, 2008; Gómez-Olivencia et al., 2009) nor to a high-protein diet (Ben-Dor et al., 2016), as previously suggested. To the contrary, this morphotype would be suitable for a great span of temperatures and environments. This is in line with previous research on other body parts (Weaver, 2009; Gavan, 2018) and strengthens the idea proposed by Churchill (2006) that similarities between the Neanderthal and cold-adapted *H. sapiens* bauplan would have been reached by equifinality. As a final point, it is worth mentioning that even though the Neanderthal ribcage may be essentially primitive (Gómez-Olivencia et al., 2009, 2018; Bastir et al., 2020), no shape similarities have yet been found between Neanderthals and other hominins dated before the Upper Pleistocene (Bastir et al., 2020, 2022). Thus, the possible evolutionary processes (selective or not) that have shaped the Neanderthal thorax are currently unknown.

## 5. Conclusions

Shanidar 3 shows the stocky 'bell-shaped' ribcage typically described for Neanderthals, characterized by a mediolaterally and anteroposteriorly expanded lower thorax and less rib torsion than in *H. sapiens*. In fact, the shapes of both Shanidar 3 and Kebara 2 ribcages cluster apart from *H. sapiens*, being, however, closer to cold-adapted individuals. Based on centroid size, the ribcage size of Shanidar 3 and Kebara 2 is not especially different from that of cold-

adapted *H. sapiens*, given that significant differences were found only between Neanderthals and temperate/tropical recent humans. As expected, there is an allometric relationship between size and shape that suggests Neanderthals had larger and stockier ribcages than *H. sapiens*, although they overlap in their ranges of variation. Finally, ribcage similarities found between Levantine Neanderthals, Shanidar 3, and Kebara 2 question the traditional assertion of a cold-adapted bauplan in *H. neanderthalensis*.

## Author contributions

**José M. López-Rey:** Writing – review & editing, Writing – original draft, Visualization, Validation, Software, Methodology, Investigation, Formal analysis, Conceptualization. **Daniel García-Martínez:** Writing – review & editing, Visualization, Validation, Supervision, Software, Methodology, Conceptualization. **Markus Bastir:** Writing – review & editing, Supervision, Project administration, Funding acquisition, Conceptualization.

## Data availability statement

The sample housed at the Musée de l'Homme (Paris) must be requested through that institution. The rest of the data that support the findings of this study are available from the corresponding author upon reasonable request. The 3D model of the Shanidar 3 reconstructed ribcage can be downloaded and visualized freely using the following links: <https://digital.csic.es/handle/10261/372005> and <https://hdl.handle.net/20.500.14352/110866>.

## Declaration of competing interest

None of the authors and acknowledged researchers of this publication state any conflict of interest.

## Acknowledgments

We would like to thank Matt Tocheri the access to the Shanidar 3 costovertebral material. We also would like to acknowledge the following researchers and technicians for their help in accessing and scanning the *Homo sapiens* sample: Ashley Hammond, Niels Lynnerup, Manuel D. D'Angelo del Campo, Chiara Villa, Martin Friess, Liliana Huet, Véronique Laborde, Bernardo Perea, Maria Teresa Ferreira, Miguel Almeida, Luis Ríos, Jorge Sanz, and Mar Casquero. This research was supported by grant PRE2021-097584 to J.M.L.-R. and grant PID2020-115854GB-I00 to M.B., funded by MCIN/AEI/10.13039/501100011033 of the Spanish Ministry of Science and Innovation.

## Appendix A. Supplementary data

Supplementary data to this article can be found online at <https://doi.org/10.1016/j.jhevol.2024.103629>.

## References

- Abdel-Maksoud, G., Kira, H.E.S., Mohamed, W.S., 2022. Consolidation of fragile archaeological bone artifacts: A review. *Egypt. J. Chem.* 65, 1065–1080. <https://doi.org/10.21608/EJCHEM.2022.158706.6860>.
- Arensburg, B., 1991. The vertebral column, thoracic cage and hyoid bone. In: BarYosef, O., Vandermeersch, B. (Eds.), *Le squelette mouestérien de Kébara 2*. Editions du CNRS, Paris, pp. 113–146.
- Ayalon, A., Inbar, O., Bar-Or, O., 1974. Relationships among measurements of explosive strength and anaerobic power. In: Nelson, R.C., Morehouse, C.A. (Eds.), *Biomechanics IV. International Series on Sport Sciences*. Palgrave, London, pp. 572–577.
- Bar-Matthews, M., Keinan, J., Ayalon, A., 2019. Hydro-climate research of the late Quaternary of the Eastern Mediterranean-Levant region based on speleothems

- research—A review. *Quat. Sci. Rev.* 221, 105872. <https://doi.org/10.1016/j.quascirev.2019.105872>.
- Bastir, M., 2008. A systems-model for the morphological analysis of integration and modularity in human craniofacial evolution. *J. Anthropol. Sci.* 86, 37–58.
- Bastir, M., 2019. Big choanae, larger face: Scaling patterns between cranial airways in modern humans and African apes and their significance in Middle and Late Pleistocene hominin facial evolution. *Bull. Mem. Soc. Anthropol. Paris* 31 (1–2), 5–13. <https://doi.org/10.3166/bmsap-2019-0055>.
- Bastir, M., Martínez, D.G., Rios, L., Higuero, A., Barash, A., Martelli, S., García Tabertero, A., Estalrrich, A., Huguet, R., de la Rasilla, M., Rosas, A., 2017a. Three-dimensional morphometrics of thoracic vertebrae in neandertals and the fossil evidence from El Sidrón (Asturias, Northern Spain). *J. Hum. Evol.* 108, 47–61. <https://doi.org/10.1016/j.jhevol.2017.03.008>.
- Bastir, M., García-Martínez, D., Torres-Tamayo, N., Sanchis-Gimeno, J.A., O'Higgins, P., Utrilla, C., Torres-Sánchez, I., García Río, F., 2017b. In vivo 3D analysis of thoracic kinematics: Changes in size and shape during breathing and their implications for respiratory function in recent humans and fossil hominins. *Anat. Rec.* 300, 255–264. <https://doi.org/10.1002/ar.23503>.
- Bastir, M., Torres-Tamayo, N., Palancar, C.A., Lois-Zlolniski, S., García-Martínez, D., Riesco-López, A., Vidal, D., Blanco-Pérez, E., Barash, A., Nalla, S., Martelli, S., Sanchis-Gimeno, J.A., Schlager, S., 2019. Geometric morphometric studies in the human spine. In: Been, E., Gómez-Olivencia, A., Kramer, P.A. (Eds.), *Spinal Evolution: Morphology, Function, and Pathology of the Spine in Hominoid Evolution*. Springer, Cham, pp. 341–360.
- Bastir, M., García-Martínez, D., Torres-Tamayo, N., Palancar, C.A., Beyer, B., Barash, A., Villa, C., Sanchis-Gimeno, J.A., Riesco-Lopez, A., Nalla, S., Torres-Sanchez, I., García-Río, F., Been, E., Gomez-Olivencia, A., Haeusler, M., Williams, S.A., Spoor, F., 2020. Rib cage anatomy in *Homo erectus* suggests a recent evolutionary origin of the studied upper diaphragms. *Nat. Ecol. Evol.* 4, 1178–1187. <https://doi.org/10.1038/s41559-020-1240-4>.
- Bastir, M., Sanz-Prieto, D., López-Rey, J.M., Palancar, C.A., Gómez-Recio, M., López-Cano, M., González-Ruiz, J.M., Pérez-Ramos, A., Burgos, M.A., Beyer, B., García-Martínez, D., 2022. The evolution, form and function of the human respiratory system. *J. Anthropol. Sci.* 100, 141–172. <https://doi.org/10.4436/jASS.10014>.
- Been, E., Waintraub, T., Gómez-Olivencia, A., Kalichman, L., Kramer, P.A., Shefi, S., Soudack, M., Barash, A., 2019. How to build a 3D model of a fossil hominin vertebral spine based on osseous material. In: Been, E., Gómez-Olivencia, A., Kramer, P.A. (Eds.), *Spinal Evolution: Morphology, Function, and Pathology of the Spine in Hominoid Evolution*. Springer, Cham, pp. 341–360.
- Ben-Dor, M., Gopher, A., Barkai, R., 2016. Neandertals' large lower thorax may represent adaptation to high protein diet. *Am. J. Phys. Anthropol.* 160, 367–378. <https://doi.org/10.1002/ajpa.22981>.
- Bramble, D.M., Lieberman, D.E., 2004. Endurance running and the evolution of *Homo*. *Nature* 432, 345–352. <https://doi.org/10.1038/nature03052>.
- Churchill, S.E., 2006. Bioenergetic perspectives on Neanderthal thermoregulatory and activity budgets. In: Hublin, J.J., Harvati, K., Harrison, T. (Eds.), *Neandertals Revisited: New Approaches and Perspectives*. Springer, Dordrecht, pp. 113–133. [https://doi.org/10.1007/978-1-4020-5121-0\\_7](https://doi.org/10.1007/978-1-4020-5121-0_7).
- Franciscus, R.G., Churchill, S.E., 2002. The costal skeleton of Shanidar 3 and a reappraisal of Neandertal thoracic morphology. *J. Hum. Evol.* 42, 303–356. <https://doi.org/10.1006/jhev.2001.0528>.
- Frumkin, A., Bar-Yosef, O., Schwarcz, H.P., 2011. Possible paleohydrologic and paleoclimatic effects on hominin migration and occupation of the Levantine Middle Paleolithic. *J. Hum. Evol.* 60, 437–451. <https://doi.org/10.1016/j.jhevol.2010.03.010>.
- García-Martínez, D., Barash, A., Recheis, W., Utrilla, C., Sánchez, I.T., Río, F.G., Bastir, M., 2014. On the chest size of Kebara 2. *J. Hum. Evol.* 70, 69–72. <https://doi.org/10.1016/j.jhevol.2014.02.003>.
- García-Martínez, D., Bastir, M., Huguet, R., Estalrrich, A., García-Tabertero, A., Ríos, L., Cunha, E., de la Rasilla, M., Rosas, A., 2017. The costal remains of the El Sidrón Neandertal site (Asturias, northern Spain) and their importance for understanding Neandertal thorax morphology. *J. Hum. Evol.* 111, 85–101. <https://doi.org/10.1016/j.jhevol.2017.06.003>.
- García-Martínez, D., Radović, D., Radović, J., Cofran, Z., Rosas, A., Bastir, M., 2018a. Over 100 years of Krapina: New insights into the Neandertal thorax from the study of rib cross-sectional morphology. *J. Hum. Evol.* 122, 124–132. <https://doi.org/10.1016/j.jhevol.2018.05.009>.
- García-Martínez, D., Torres-Tamayo, N., Torres-Sánchez, I., García-Río, F., Rosas, A., Bastir, M., 2018b. Ribcage measurements indicate greater lung capacity in Neandertals and Lower Pleistocene hominins compared to modern humans. *Commun. Biol.* 1, 117. <https://doi.org/10.1038/s42003-018-0125-4>.
- García-Martínez, D., Riesco, A., Bastir, M., 2018c. Missing element estimation in sequential anatomical structures: The case of the human thoracic vertebrae and its potential application to the fossil record. In: Rissech, C., Lloveras, L., Nadal, J., Fullola, J.M. (Eds.), *Geometric Morphometrics: Trends in Biology, Paleobiology and Archaeology*. SERP, Seminari d'Estudis i Recerques Prehistòriques. Universitat de Barcelona, Societat Catalana d'Arqueologia, pp. 93–97.
- García-Martínez, D., Bastir, M., Gómez-Olivencia, A., Maureille, B., Golovanova, L., Doronichev, V., Akazawa, T., Kondo, O., Ishida, H., Gascho, D., Zollikofer, C.P.E., Ponce de León, M., Heuzé, Y., 2020. Early development of the Neandertal ribcage reveals a different body shape at birth compared to modern humans. *Sci. Adv.* 6, eabb4377. <https://doi.org/10.1126/sciadv.abb4377>.
- García-Martínez, D., Recheis, W., Bastir, M., 2016. Ontogeny of 3D rib curvature and its importance for the understanding of human thorax development. *Am. J. Phys. Anthropol.* 159, 423–431. <https://doi.org/10.1002/ajpa.22893>.
- Gavan, Z., 2018. Neandertals (*Homo neanderthalensis*): An adaptive paradox. *The Human Voyage* 2, 1–7.
- Gómez-Olivencia, A., Eaves-Johnson, K.L., Franciscus, R.G., Carretero, J.M., Arsuaga, J.L., 2009. Kebara 2: New insights regarding the most complete Neandertal thorax. *J. Hum. Evol.* 57, 75–90. <https://doi.org/10.1016/j.jhevol.2009.02.009>.
- Gómez-Olivencia, A., Barash, A., García-Martínez, D., Arlegi, M., Kramer, P., Bastir, M., Been, E., 2018. 3D virtual reconstruction of the Kebara 2 Neandertal thorax. *Nat. Commun.* 9, 4387. <https://doi.org/10.1038/s41467-018-06803-z>.
- Graeber, G.M., Nazim, M., 2007. The anatomy of the ribs and the sternum and their relationship to chest wall structure and function. *Thorac. Surg. Clin.* 17, 473–489. <https://doi.org/10.1016/j.thorsurg.2006.12.010>.
- Hardy, K., Bocherens, H., Miller, J.B., Copeland, L., 2022. Reconstructing Neandertal diet: The case for carbohydrates. *J. Hum. Evol.* 162, 103105. <https://doi.org/10.1016/j.jhevol.2021.103105>.
- Helmens, K.F., 2014. The Last Interglacial–Glacial cycle (MIS 5–2) re-examined based on long proxy records from central and northern Europe. *Quat. Sci. Rev.* 86, 115–143. <https://doi.org/10.1016/j.quascirev.2013.12.012>.
- Henry, A.G., Brooks, A.S., Piperno, D.R., 2011. Microfossils in calculus demonstrate consumption of plants and cooked foods in Neandertal diets (Shanidar III, Iraq; Spy I and II, Belgium). *Proc. Natl. Acad. Sci. U.S.A.* 108, 486–491. <https://doi.org/10.1073/pnas.1016868108>.
- Karasik, D., Arensburg, B., Tillier, A.M., Pavlovsky, O.M., 1998. Skeletal age assessment of fossil hominids. *J. Archaeol. Sci.* 25, 689–696. <https://doi.org/10.1006/jasc.1997.0264>.
- Lieberman, D.E., Bramble, D.M., 2007. The evolution of marathon running: capabilities in humans. *Sports Med.* 37, 288–290. <https://doi.org/10.2165/00007256-200737040-00004>.
- LoMauro, A., Aliverti, A., 2018. Sex differences in respiratory function. *Breathe* 14, 131–140. <https://doi.org/10.1183/20734735.000318>.
- López-Rey, J.M., García-Martínez, D., Martelli, S., Beyer, B., Palancar, C.A., Torres-Sánchez, I., García-Río, F., Bastir, M., 2023. Estimation of the upper diaphragm in KNM-WT 15000 (*Homo erectus* s.l.) and Kebara 2 (*Homo neanderthalensis*) using a *Homo sapiens* model. *J. Hum. Evol.* 185, 103442. <https://doi.org/10.1016/j.jhevol.2023.103442>.
- López-Rey, J.M., D'Angelo del Campo, M.D., Seldes, V., García-Martínez, D., Bastir, M., 2024a. Eco-geographic and sexual variations in the *H. sapiens* ribcage. *Evol. Anthropol.* e22040. <https://doi.org/10.1002/evan.22040>.
- López-Rey, J.M., García-Martínez, D., Bastir, M., 2024b. How to make a digital reconstruction of the human ribcage. *J. Anat.* 245, 27–34. <https://doi.org/10.1111/joa.14022>.
- Manifold, B.M., 2012. Intrinsic and extrinsic factors involved in the preservation of non-adult skeletal remains in archaeology and forensic science. *Bull. Int. Assoc. Paleodontology* 6, 51–69.
- Müller, U.C., Pross, J., Tzedakis, P.C., Gamble, C., Kotthoff, U., Schmiedl, G., Wulf, S., Christanis, K., 2011. The role of climate in the spread of modern humans into Europe. *Quat. Sci. Rev.* 30 (3–4), 273–279. <https://doi.org/10.1016/j.quascirev.2010.11.016>.
- Ocobock, C., Lacy, S., Niclou, A., 2021. Between a rock and a cold place: Neandertal biocultural cold adaptations. *Evol. Anthropol.* 30, 262–279. <https://doi.org/10.1002/evan.21894>.
- Pomeroy, E., 2023. The different adaptive trajectories in Neandertals and *Homo sapiens* and their implications for contemporary human physiological variation. *Comp. Biochem. Physiol. Mol. Integr. Physiol.* 280, 111420. <https://doi.org/10.1016/j.cbpa.2023.111420>.
- Pomeroy, E., Bennett, P., Hunt, C.O., Reynolds, T., Farr, L., Frouin, M., Holman, J., Lane, R., French, C., Barker, G., 2020. New Neandertal remains associated with the 'flower burial' at Shanidar Cave. *Antiquity* 94, 11–26. <https://doi.org/10.15184/aqy.2019.207>.
- Raichlen, D.A., Armstrong, H., Lieberman, D.E., 2011. Calcaneus length determines running economy: Implications for endurance running performance in modern humans and Neandertals. *J. Hum. Evol.* 60, 299–308. <https://doi.org/10.1016/j.jhevol.2010.11.002>.
- Richtsmeier, J.T., Burke DeLeon, V., Lele, S.R., 2002. The promise of geometric morphometrics. *Am. J. Phys. Anthropol.* 119, 63–91. <https://doi.org/10.1002/ajpa.10174>.
- Sawyer, G.J., Maley, B., 2005. Neandertal reconstructed. *Anat. Rec.* 283, 23–31. <https://doi.org/10.1002/ar.b.20057>.
- Schmid, P., Churchill, S.E., Nalla, S., Weissen, E., Carlson, K.J., de Ruiter, D.J., Berger, L.R., 2013. Mosaic morphology in the thorax of *Australopithecus sediba*. *Science* 340, 1234598. <https://doi.org/10.1126/science.1234598>.
- Schotsmans, E.M., Márquez-Grant, N., Forbes, S.L. (Eds.), 2017. *Taphonomy of Human Remains: Forensic Analysis of the Dead and the Depositional Environment*. John Wiley & Sons, Chichester.
- Stewart, J.R., García-Rodríguez, O., Knul, M.V., Sewell, L., Montgomery, H., Thomas, M.G., Diekmann, Y., 2019. Palaeoecological and genetic evidence for Neandertal power locomotion as an adaptation to a woodland environment. *Quat. Sci. Rev.* 217, 310–315. <https://doi.org/10.1016/j.quascirev.2018.12.023>.
- Trinkaus, E., Thompson, D.D., 1987. Femoral diaphyseal histomorphometric age determinations for the Shanidar 3, 4, 5, and 6 Neandertals and Neandertal longevity. *Am. J. Phys. Anthropol.* 72, 123–129. <https://doi.org/10.1002/ajpa.1330720115>.
- Wanger, J., Clausen, J.L., Coates, A., Pedersen, O.F., Brusasco, V., Burgos, F., Casaburi, R., Crapo, R., Enright, P., van der Grinten, C.P.M., Gustafsson, P., Hankinson, J., Jensen, R., Johnson, D., MacIntyre, N., McKay, R., Miller, M.R., Navajas, D., Pellegrino, R., Viegi, G., 2005. Standardisation of the measurement

- of lung volumes. *Eur. Respir. J.* 26, 511–522. <https://doi.org/10.1183/09031936.05.00035005>.
- Weaver, T.D., Roseman, C.C., Stringer, C.B., 2007. Were Neandertal and modern human cranial differences produced by natural selection or genetic drift? *J. Hum. Evol.* 53, 135–145. <https://doi.org/10.1016/j.jhevol.2007.03.001>.
- Weinstein, K.J., 2008. Thoracic morphology in Near Eastern Neandertals and early modern humans compared with recent modern humans from high and low altitudes. *J. Hum. Evol.* 54, 287–295. <https://doi.org/10.1016/j.jhevol.2007.08.010>.
- Wickham, H., 2016. *ggplot2: Elegant Graphics for Data Analysis*. Springer-Verlag, New York.
- Zappalá, M., Lightbourne, S., Heneghan, N.R., 2021. The relationship between thoracic kyphosis and age, and normative values across age groups: A systematic review of healthy adults. *J. Orthop. Surg. Res.* 16, 447. <https://doi.org/10.1186/s13018-021-02592-2>.